

Contributions of a weed; Microwave assisted green synthesis of silver nanoparticles using morning glory (*Ipomoea* spp.) for the assessment of its antioxidant, antibacterial and photocatalytic activity

Ramlah Mohamed Kamal¹ and Mathivathani Kandiah^{1*}

¹School of Science, Business Management School (BMS), Sri Lanka

*mathi@bms.ac.lk

Abstract

The *Ipomoea* spp. is a common weed which has untapped potential for the scientifically significant green synthesis silver nanoparticles (AgNPs). AgNPs have multiple benefits in fields including medicine and environmental clean-up. In this study, eco-friendly water-based extraction was carried out on the leaves of five different *Ipomoea* spp. The synthesis of AgNPs was attempted using the extracts. *Ipomoea lacunosa* (S3) AgNPs were successfully generated through microwave assisted synthesis. The formation of AgNPs caused the solution to deepen in colour and resulted in a peak of 420nm under UV-Vis spectroscopy. This peak corresponded to the surface plasmon resonance (SPR) peak of AgNPs. The S3AgNPs, characterized by Scanning Electron Microscopy, were spherical and of 60nm in diameter. Furthermore, the antioxidant, antibacterial and photocatalytic activity of the S3AgNPs were compared against *I. aquatica*, *I. cairica*, *I. pes-caprae* and *I. purpurea* water extracts. The S3AgNPs showed elevated activity as opposed to the water extracts in the Total Flavonoid Content, Total Phenolic Content, Total Antioxidant Content and DPPH assays. It had an IC₅₀ of 20.3% in the DPPH assay. The S3AgNPs demonstrated potent antibacterial activity against the Gram-negative *Escherichia coli* and the Gram-positive *Staphylococcus aureus* as opposed to the water extracts. A higher zone of inhibition was observed for the *S. aureus* compared to *E. coli*. In the presence of sodium borohydride, 100ppm of S3AgNPs degraded 94% of Methylene blue dye in 240 minutes. The implications of this research are widespread and can be used to develop novel antibiotics, antioxidants and water treatment compounds.

Keywords: silver nanoparticles, *Ipomoea* spp., microwave-assisted, antioxidant activity, photocatalytic activity, antibacterial activity

1. Introduction

Nanotechnology is a thriving and relatively novel field of science which deals with the synthesis of particles sized between 1-100nm. The use of nanoparticles is gaining momentum as they are potent in multiple fields including medicine, engineering, electronics and environmental clean-up due to their high surface area to volume ratio. Nanoparticles are produced using two principle approaches. The top-down approach begins with larger particles which are consequently degenerated in size until they form nanoparticles. The bottom-up approach causes the proliferation of atomic and molecular particles to form larger nanosized particles. The

three primary methods of synthesis are through chemical, physical and biological processes.¹

Silver nanoparticles (AgNPs), as opposed to other metallic nanoparticles remain in the limelight due to its non-toxicity, well-documented antimicrobial activity, catalytic properties, and its great thermal and electrical conductivity. These merits contribute to AgNPs having the highest marketing value of all nanoparticles, and this trend is expected to grow exponentially.¹ It has been forecasted that by 2025, the global market value of AgNPs would reach \$USD 98 billion.^{2,3} As the use of AgNPs increases, much focus has been placed on synthesising them with minimal environmental impact. The green synthesis of nanoparticles

utilises plant or microorganism-based protocols, allowing the use of toxic solvents and the formation of harmful by-products to be circumvented.⁴ Plant based synthesis of AgNPs gives rise to undisrupted surfaces, unlike those formed using the top-down approach and provides a more economical and simpler alternative to using microorganisms. Plant extracts reduce silver ions to metallic silver, effectively building up nanoparticles from the atomic scale until they reach the nanoscale. The extracts also contain polyphenols, amino acids and vitamins which act as capping agents that regulate the size of the particles, stabilizing them and preventing agglomeration.⁵

The primary heating techniques used in plant-mediated synthesis of nanoparticles are mild-heat and high-heat synthesis. Although the choice of conventional heating or microwave irradiation is predominantly governed by the plant material, microwave assisted heating (MAS) is energy efficient, faster, reduces agglomeration and produces nanoparticles with smaller size variation.⁶

The *Ipomoea* spp. is the largest genus classified under the family of *Convolvulaceae*, which contains flowering plants commonly known as the Morning Glory.⁷ The genus grows abundantly in the tropics and some temperate regions and has been termed a weed as a result. The trumpet shaped showy flowers have been grown as an ornamental while some the seeds of some species show psychedelic properties. The leaves of *Ipomoea aquatica* is consumed in Sri Lanka, South-East Asia and China for its high nutritional value. The leaves, seeds and roots of multiple species are also well known for ethnic medicinal treatments, where they have been used as a hypoglycaemic, purgative, anti-arthritis, anti-microbial and anti-inflammatory compound among others.⁸ Five different species of *Ipomoea* AgNPs are comparatively analysed in this study, *I. aquatica*, *I. cairica*, *I. lacunosa*, *I. pes-caprae* and *I. purpurea*.

The spread of resistant bacteria remains a threat only intensified by the emergence of multi-drug resistant super bacteria. Silver is an age known antimicrobial agent and coupling it with the efficacy of nanoparticles makes it a potential weapon against bacteria. Due to their size, AgNPs can easily gain access to cells to exert antibacterial effects and as they are not known to induce resistance, they remain an attractive choice for antibacterials.⁹

The contribution of azo dyes to environmental pollution is significant as they are released by multiple industries from textiles to printing. These dyes are persistent compounds which can accumulate in organisms and can have harmful and even carcinogenic effects.⁹ Standard effluent treatments only achieve substandard efficiency and create sludge with amine residues whereas AgNPs synthesised via the green route have the additional advantage of lower risk in terms of long-term toxicity as they do not persist in the environment unlike conventional dye degrading treatments.¹⁰⁻¹²

The elucidation of the exact mechanisms of the photocatalytic effect of AgNPs is still in progress and the current consensus is that electrons absorb 2.7-3.03 eV of energy from the UV-Vis spectral range, exciting them from the valence band to the conductance band whilst creating holes.¹³ This leads to a photo-redox reaction which reduces oxygen to oxygen radicals and oxidises hydroxide ions to hydroxide radicals.¹⁴ The free radicals can then attack and degrade azo dyes like methylene blue. The phytoremediation expected from the *Ipomoea* extracts coupled with the potency of AgNPs could lead to synergistic effects in the combined photocatalytic potential of *Ipomoea* AgNPs.

The balance between free radicals (FRs) and antioxidants in the human body is a precarious one. FRs extend a three-pronged attack on proteins, nucleic acids and lipids leading to cell damage and ultimately cell death due to oxidative stress.¹⁵⁻¹⁷

Oxidative stress also plays a role in the progression of diabetes, cancer, cardiovascular diseases, neurodegenerative conditions and aging. Although the body is equipped to neutralise endogenously produced FRs, exposure to stressors like radiation, pollution heavy metals and processed food can disturb this fine balance as they encourage higher FR production rates.¹⁸ The free radical scavenging activity of antioxidants takes place through the transfer of an electron or a hydrogen atom.^{19,20} This ability of antioxidants to counterattack the detrimental effects of FR forms the basis for gauging antioxidant capacities of the synthesised *auoea* nanoparticles.

Previous research on the different species of *Ipomoea* have proved their high potential as precursors for AgNPs as they contain a high concentration of phytochemicals and antioxidants.²¹⁻²³ Therefore, this study focuses on the synthesis of five varieties of *Ipomoea* AgNPs for the determination of its antioxidant, antibacterial and photocatalytic activities. The assessment of antioxidant capacity would be based on the TAC, TPC, TFC and DDPH assays while the antibacterial activity will be tested using well diffusion against *S. aureus* and *E. coli*. The photocatalytic activity will be judged using methylene blue as a model dye. The outcomes of the research are expected to contribute towards the advancements in disease treatment and water effluent treatment.

2. Methodology

2.1. Preparation of leaf extracts. Leaf samples of *I. aquatica* (S1), *I. cairica* (S2), *I. lacunosa* (S3), *I. pes-caprae* (S4) and *I. purpurea* (S5) were washed and shade dried. The dried leaf samples were ground to fine particles. Then 2.0g of each sample was added to 50mL of distilled water. The mixture was incubated at 95°C in a dry hot air oven for 20 minutes. The cooled extracts were subsequently filtered using Whatman No.1 filter paper and stored at 4°C till required.²⁴

2.2 Optimization of conditions for the synthesis of nanoparticles. 9mL of 1mM AgNO₃ was added dropwise to 1mL of *Ipomoea* extract. The prepared solutions were then heated in a microwave at 140W, 364W and 511W for 2.5 and 5 minute intervals. The absorbance values were taken between 300-540nm using a UV spectrophotometer.²⁴

2.3 Phytochemical analysis. The protocols detailed by Ravi and Krishnamurthy was followed to build a phytochemical profile consisting of alkaloids, anthocyanins, carbohydrates, coumarin, quinones, saponins, tannins and terpenoids.²⁵

2.4 Dilution of the samples. The extracts and S3AgNP samples were diluted in a 1:15 ratio using distilled water.

2.5 Antioxidant Assays: The diluted water extracts and AgNPs were used in the following assays.

2.5.1 Total Flavonoid Content (TFC) Assay. To 1.5mL of sample, 0.2mL of 10% (w/v) AlCl₃ and 0.2mL of 1M potassium acetate were added. The mixture was left to rest at room temperature for 30 minutes, Triplicates were prepared and left at room temperature for 30 minutes. The absorbance was measured in triplicates using spectrophotometer against water as a blank at 415 nm. The concentration was expressed in equivalents of Quercetin acid in gQE/100g.²⁶

2.5.2 Total Phenolic Content (TPC) Assay. To 0.4mL of the sample, an equal volume of 10% (v/v) Folin-Ciocalteu reagent was added along with 1.25mL of 7.5% (v/v) Na₂CO₃. The mixture was incubated for 2 hours at room temperature. The absorbance was measured in triplicates using spectrophotometer against water as a blank at 765 nm. The concentration was expressed in equivalents of Gallic acid in mgGAE/100g.²⁶

2.5.3 Total Antioxidant Capacity (TAC) Assay. To prepare the phosphomolybdenum reagent, (0.6M Sulfuric acid, 28mM sodium phosphate and 4mM ammonium molybdate in a 1:1:1 ratio)

were mixed. 0.5mL of the reagent was added to 1.5mL of the samples and incubated at 95°C for 90 minutes. The absorbance was then read in triplicates using spectrophotometer against water as a blank at 695nm. The concentration was expressed in equivalents of ascorbic acid in µgAAE/100g.²⁶

2.5.4 DPPH Assay. The plant extracts and S3AgNPs were diluted with distilled water to achieve a concentration series of 100%, 80%, 60% 40% and 20%. 1mL of the sample was reacted with 2mL of 0.1mM DPPH in methanol and the absorbance was measured in triplicates using spectrophotometer against methanol as a blank. The radical scavenging activity was calculated as follows:

$$\% \text{ Activity} = \frac{A_{DPPH} - A_{\text{sample}}}{A_{DPPH}} \times 100$$

Where A_{sample} was the absorbance of the sample and A_{DPPH} was the absorbance of the DPPH stock solution.²⁶

2.6. Antibacterial activity. Isolated colonies of *E. coli* and *S. aureus* were inoculated into 0.9% saline (w/v) to match the turbidity of a 0.5% McFarland standard. Mueller Hinton agar plates were inoculated with the two bacterial species and wells were created using a 10mm pipette tip bore. 1mL of the water extracts and the S3AgNPs was slow dried at 45°C in an oven until they evaporated. The dried samples were rehydrated by the addition of 200µL of distilled water and 50µL was loaded into each of the respective wells. For the negative control, 0.9% of saline was used while gentamicin disks were placed as positive controls. The plates were sealed and incubated upright at 37°C for 24 hours. The zones of inhibition were measured in centimetres.

2.7. Analysis of the photocatalytic activity. 10 mg/L methylene blue was prepared, and an absorbance curve was plotted between 340-780nm using a UV spectrophotometer. Dye solutions containing 10,100 and 500ppm of S3AgNPs were left under direct sunlight and

absorbance readings were taken at specified time intervals. This was repeated with the addition of 10µL of 0.2M NaBH₄.²⁷

2.8. SEM Analysis. The S3AgNPs were characterized at the Sri Lanka Institute of Nanotechnology (SLINTEC), Homagama using a Hitachi SU66600 SEM.

2.9. Statistical Analysis. Statistical analysis of the data was computed using Excel® for Microsoft 365 to obtain ONE-way ANOVA and t-tests while correlation graphs were plotted using IBM® SPSS® Statistics, version 21. All statistical tests were significant at a minimum p value of 0.05.

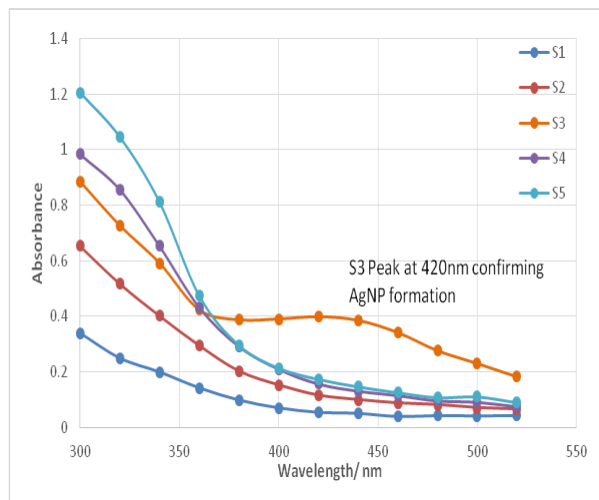
3. Results and Discussion

The colour of the solution gradually changed from pale yellow brown to deep red brown indicating the formation of AgNPs. Only S3 generated a single distinct peak at 420nm at 140W (2.5 mins), 364 (2.5 and 5.0 mins) and 511W (5.0 mins) giving a preliminary confirmation of AgNP synthesis. This peak is characteristic of AgNPs and corresponds to its surface plasmon resonance (Figure 1). The other samples had no peaks indicating non-formation of AgNPs.

The green synthesis of AgNPs has a plethora of benefits over conventional chemical methods in terms of environmentally friendliness, economy and yield. It remains a highly attractive research field with plant origins offering higher control and flexibility in terms of size and morphology of prepared particles.²⁸ The use of water as an alternative to organic solvents during the extraction process maintains this eco-friendliness of the protocol.²⁹ In this research we explored the synthesis and properties of nanoparticles from five different species of *Ipomoea*. The utilization of the *Ipomoea* species for the synthesis of nanoparticles can carry multiple advantages as the species is a pernicious weed with no competing uses. This could be an

efficient way to ensure mechanical movement of the plant and control its spread.³⁰

Figure 1. Absorbance vs wavelength graph for UV-Vis characterisation of silver nanoparticles at



140W for 2.5 minutes.

The analysis of spectrophotometric curves showed that *Ipomoea lacunosa* (S3) was the only species that was able to successfully synthesise AgNPs. However, AgNPs from the other species of *Ipomoea* have been successfully synthesized in other studies and the reasons behind the absence of nanoparticles in this study can be conjectured on. This could be because S3 had more stable and higher content of reducing agents like proteins, amino acids, polysaccharides, terpenoids and vitamins.³¹ In addition, S3 was the only sample which had all the phytochemicals tested. All the samples tested positive for tannins and quinones while carbohydrates were seen in none.

The microwave assisted synthesis (MAS) of AgNPs is a one pot reaction that combines the nucleation and growth phases in a single efficient reaction.³² The alternate kinetics followed by MAS allow for a shorter heating time making the process highly efficient and even results in a higher yield.³³ Additional benefits of MAS include an increased uniformity and a greater control of nanoparticle morphology size and

crystallinity.³⁴ Comparative studies done on noble metal NPs have demonstrated that MAS of NPs result in an elevated catalytic activity as opposed to those synthesised using conventional heat induced methods.³⁵

The UV-vis spectrum, in addition to providing preliminary details of nanoparticle synthesis was also used to determine the optical properties of the AgNPs. The conductivity of the AgNPs can be gauged by calculation of the band gap energy. The band gap is defined as the minimum energy required for an electron to transition from the valence band to the conduction band. The band gap energies can differentiate between semi-conductors, which have a band gap less than 3eV, and insulators which have a band gap greater than 4eV.

To determine the band gap of the nanoparticles the following equation was used.

$$\text{Band gap energy} = \frac{h \times c}{\lambda}$$

where h is the Planck constant, c is the speed of light and λ is the absorbance peak obtained during characterization of the nanoparticles.

Based on their band energy of 2.96eV, the S3AgNPs were classified as semiconductors. This explains their photocatalytic activity as semi-conducting nanoparticles have been shown to possess intrinsic dye degradation abilities. This property also indicates that the synthesized AgNPs can be used in biosensors, light emitting devices, electronic devices, and even solar cells. The synthesized AgNPs had a mean width of 60nm and a spherical morphology (Figure 2).

The S3AgNPs outperformed the water extracts in the TFC, TPC and TAC assays and the differences were all statistically significant (Table 1).

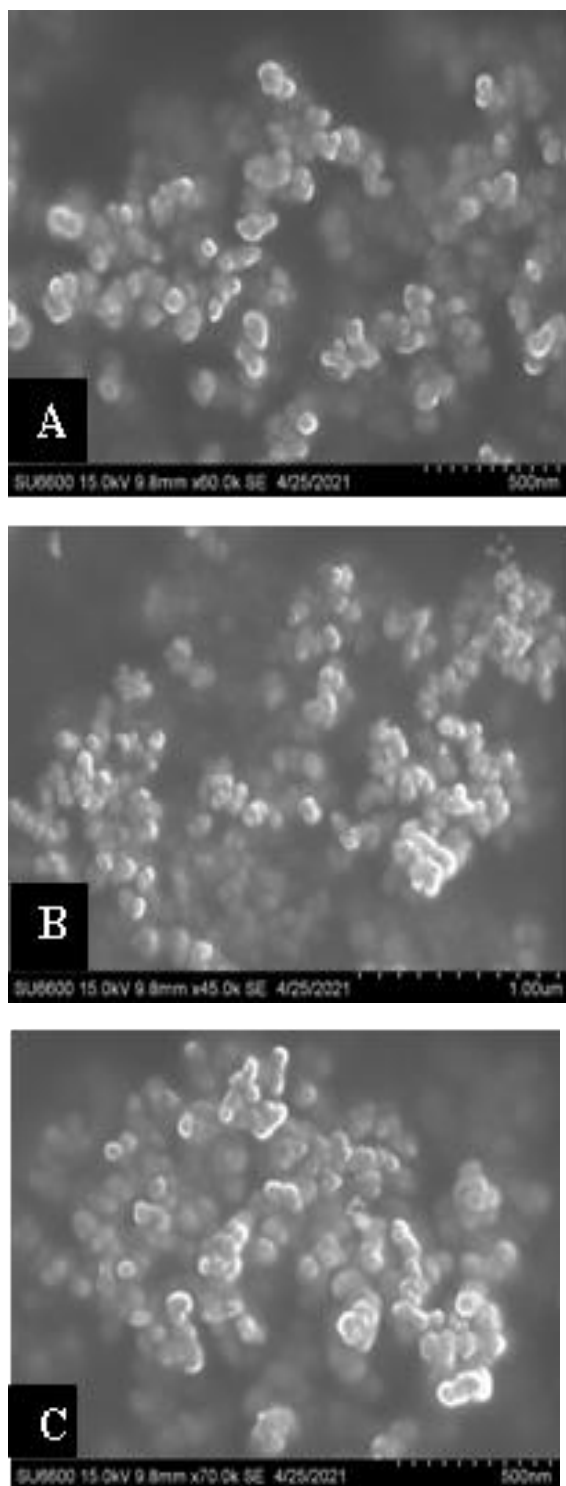


Figure 2. SEM images of S3AgNPs at different magnifications A) x60.0k B) x45.0k C) x70.0k

Table 1. The total flavonoid content, total phenolic content and the total antioxidant

capacity of the leaf water extracts and the S3AgNPs.

Sample	TFC (gQE/ 100g of sample)	TPC (mgGAE/ 100g of sample)	TAC (μ gAAE/ 100g of sample)
S1	0.83 \pm 0.06	48.21 \pm 6	9.89 \pm 1.4
S2	1.2 \pm 0.02	34.64 \pm 6.2	22.16 \pm 5.5
S3	1.74 \pm 0.14	42.86 \pm 8.5	16.7 \pm 2.7
S4	3.05 \pm 0.2	43.21 \pm 5.5	23.07 \pm 2.7
S5	3.69 \pm 0.05	42.14 \pm 10.7	39.77 \pm 1
S3AgNP	6.04 \pm 0.53	1561 \pm 257	97.72 \pm 20.5

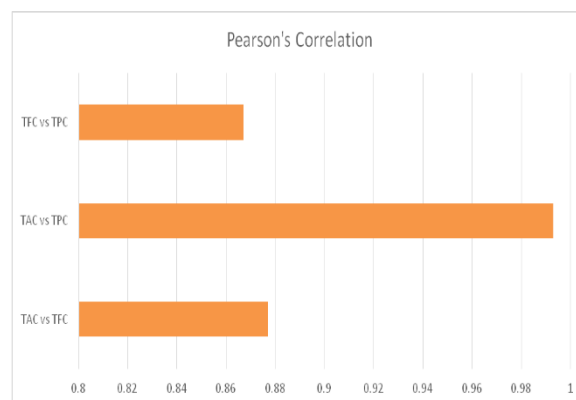


Figure 3. Pearson's correlation between the TAC, TFC and TPC assays.

The antioxidant properties of the particles were investigated using the TFC, TAC, TPC and DPPH assays. Phenols and flavonoids have optimal structures for the donation of electrons in the scavenging of free radicals making them effective antioxidants.³⁶ To elucidate which of the two contributed most towards the antioxidant properties seen, regression plots using the Pearson's correlation test were generated to obtain R values. The highest correlation was seen between the TAC and TPC assays which were a strong indication

that the antioxidant properties of the leaf extracts were primarily mediated by the phenols present (Figure 3). This deduction is in line with previous research conducted on the *Ipomoea* species.^{37,38} The phenols predominantly contributing towards the antioxidant activity could include caffeoylquinic acid derivatives.³⁹ The DPPH activities were expressed as IC₅₀ values (Table 2). The S3AgNPs had the lowest IC₅₀ demonstrating it was the highest-ranking FR scavenger and could reach 50% of maximal activity at a concentration of 20.6%. The most potent scavenger amongst the water extracts was S1 with an IC₅₀ value that was identical to previous studies.^{26,36}

Table 2. IC₅₀ of DPPH free radical scavenging activities of the leaf water extracts and S3AgNPs

Sample	IC ₅₀ (%)
S1	48.4
S2	63.6
S3	69.9
S4	75.4
S5	77.4
S3AgNPs	20.3

The S3AgNPs formed higher zones of inhibition in comparison to the leaf extracts in both *E. coli* and *S. aureus* (Figure 4). Between the bacterial species, greater antibacterial activity was observed against *S. aureus* allowing us to deduce that the *Ipomoea* species was more adept at the disruption of Gram-positive bacterial colonies. This is in agreement to other studies that have dealt with the family of *Ipomoea*.²⁴ Gram positive bacteria evolve resistant mechanisms easily and this potency of S3AgNPs against the species can be exploited to develop novel antibacterial remedies.

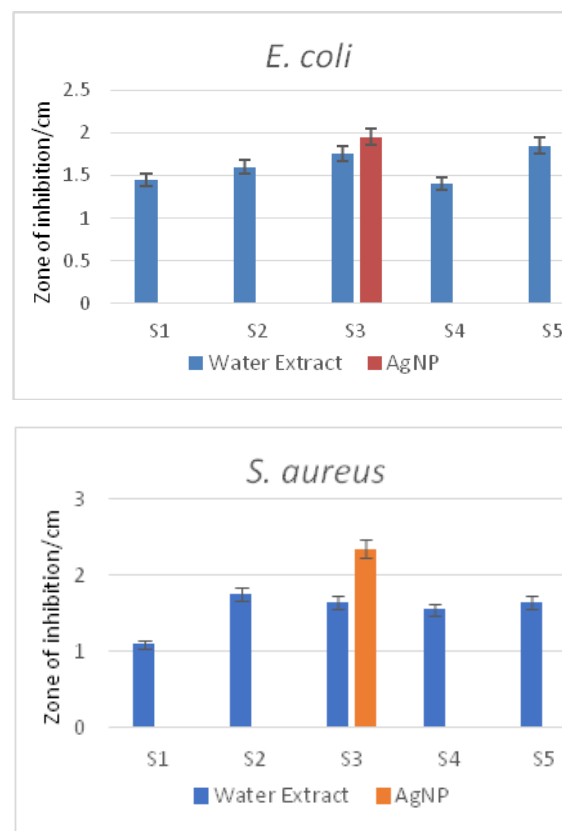


Figure 4. Diameter of the zones of inhibition in *E. coli* (left) and *S. aureus* (right) of the water extracts and S3AgNPs

In the absence of NaBH₄, the S3AgNPs were able to decrease the peak of methylene blue although no visible decolorisation took place. In the presence of NaBH₄, however, significant decolorisation was seen. Using 100ppm of AgNPs in the presence of NaBH₄ resulted in a 94% dye degradation in 240 minutes (Figure 5)

AgNPs inherently possess photocatalytic activity but the conjugation with plant extracts intensifies this effect. Compared to other metallic nanoparticles, AgNPs demonstrate greater photocatalytic strength due to its smaller band gap energy.⁴⁰ Furthermore, AgNPs have high absorption within the visible light spectrum. It therefore is a perfect candidate to exploit in the

goal of dye degradation. In this study, the S3AgNPs were exposed to different conditions in terms of concentration of the AgNPs and the presence or absence of a catalyst. In the absence of a catalyst, the S3AgNPs showed modest photocatalytic activity where the absorbance peak decreased but complete degradation was not observed. This validated the use of a catalyst for further analysis. The cationic NaBH_4 was able to cause a dramatic degradation of the dye after just 120 minutes. The kinetics of the photocatalytic activity were plotted using the equation below on the assumption that first-order kinetics were followed:

$$\ln \frac{C}{C_0} = kt$$

where C was the concentration, C_0 was the initial concentration and t was the time. Values of the rate constant (k) were obtained from the slope and are listed in Table 3.

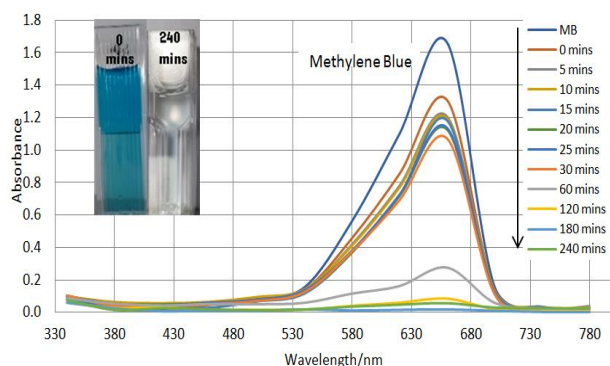


Figure 5. Photocatalytic activity of 100ppm S3AgNPs with NaBH_4

The highest rate constant obtained was for 100ppm of dye with NaBH_4 indicating that these conditions are the closest to the optimum working conditions of the synthesized S3AgNPs. In reactions which included NaBH_4 , a higher dose of AgNPs resulted in a greater photocatalytic effect. This observation was also reported in previous studies on other *Ipomoea* species. Conversely, in the absence of NaBH_4 , lower concentrations showed more enhanced activity. This observation could be due to the aggregation

of AgNPs at increasing concentration which reduces the surface area available for catalysis.

Table 3. Rate constants of the different S3AgNPs reaction mixtures

Conditions	Rate constant (k/min^{-1})
10ppm	0.0068
100ppm	0.0059
500ppm	0.0057
10ppm with NaBH_4	0.0160
100ppm with NaBH_4	0.0187

This study is the first of its kind to describe the synthesis and activity of *I. lacunosa* AgNPs. The S3AgNPs performed remarkably in the antioxidant, antibacterial and photocatalytic assays. It is hoped that these novel findings which prove the efficacy of S3AgNPs leads to their use in biomedicine, electronics and water waste treatment.

4. Conclusion

Ipomoea lacunosa silver nanoparticles were successfully synthesized using microwave assisted heating techniques. The S3AgNPs exhibited antioxidant properties that surpassed those of the leaf extracts. Similarly, they also contained antibacterial properties and demonstrated evidence of heightened action against Gram-positive bacteria. Furthermore, the photocatalytic studies highlighted the efficacy of the S3AgNPs in the degradation of azo dyes like methylene blue.

Acknowledgements

The authors would like to acknowledge Business Management School (BMS) for the opportunity to conduct the research project and the Sri Lanka Institute of Nanotechnology (SLINTEC) for allowing the use of the Hitachi SU6600 SEM.

References

- 1 B. Calderón-Jiménez, M.E. Johnson, A.R. Montoro Bustos, K.E. Murphy, M.R. Winchester and J.R. Vega Baudrit. *Frontiers in Chemistry*, 2017;**5**.
- 2 M. Jeyaraj, S. Gurunathan, M. Qasim, M-H. Kang and J-H. Kim. *Nanomaterials*, 2019;**9**:1-41.
- 3 J. Pulit-Prociak and M. Banach. *Open Chemistry*, 2016;**14**:76-91.
- 4 A. Gour and N.K. Jain, *Artificial Cells, Nanomedicine, and Biotechnology*, 2019;**47**:844-851.
- 5 M. Khan, F. Ahmad, J.T. Koivisto and M. Kellomäki. *Colloid and Interface Science Communications*, 2020;**39**:101-108.
- 6 S. Irvani, H. Korbekandi, S.V. Mirmohammadi and B. Zolfaghari. *Research in Pharmaceutical Science*. 2014;**9**:385-406.
- 7 J.R.I. Wood, P. Muñoz-Rodríguez, B.R.M. Williams and R.W. Scotland. *PhytoKeys*, 2020;**143**:1-823.
- 8 D.K. Londhe, N. Rs and A. Bhuktar. *International Journal of Trend in Scientific Research and Development*, 2017;**3**:82-84.
- 9 V.K. Balakrishnan, S. Shirin, A.M. Aman, S.R. de Solla, J. Mathieu-Denoncourt and V.S. Langlois. *Chemosphere*, 2016;**146**:206-215.
- 10 S. Marimuthu, A.J. Antonisamy, S. Malayandi, K. Rajendran, P-C. Tsai, A. Pugazhendhi and V.K. Ponnusamy. *Journal of Photochemistry and Photobiology B: Biology*, 2020;**205**:111823.
- 11 S. Sarkar, N.T. Ponce, A. Banerjee, R. Bandopadhyay, S. Rajendran and E. Lichtfouse. *Environmental Chemistry Letters*, 2020;**18**:1569-1580.
- 12 G. Crini, E. Lichtfouse, L.D. Wilson and N. Morin-Crini. *Environmental Chemistry Letters*, 2019;**17**:195-213.
- 13 A. Campos, N. Troc, E. Cottancin, M. Pellarin, H-C. Weissker, J. Lermé, M. Kociak and M. Hillenkamp. *Nature Physics*, 2019;**15**:275-280.
- 14 J. Singh and A.S. Dhaliwal. *Environmental Technology*, 2020;**41**:1520-1534.
- 15 A. Gatin, I. Billault, P. Duchambon, G. Van der Rest and C. Sicard-Roselli. *Free Radical Biology and Medicine*, 2021;**162**:461-470.
- 16 H. Zhao, M. Liu, T. Jiang, J. Xu, H. Zhang, C. Yu, Z. Liu, Y. Wang and L. Tang. *Environment International*, 2020;**139**:105672.
- 17 Á. Sánchez-Illana, S. Thayyil, P. Montaldo, D. Jenkins, G. Quintás, C. Oger, J-M. Galano, C. Vigor and G. Zastrow. *Analytica Chimica Acta*, 2017;**996**:88-97.
- 18 S.B. Lohan, D. Ivanov, N. Schöler, B. Berger, L. Zastrow, J. Lademann and M.C. Meinke. *Free Radical Biology and Medicine*, 2021;**162**:401-11.
- 19 F.N. Eze and O.F. Nwabor. *Materials Science and Engineering*, 2020;**115**:111104.
- 20 V. Rashmi, J.P. Kumar, and K.R. Sanjay. *Materials Today: Proceedings*, 2020;**43**:3635-3642.
- 21 Y.R. Im, I. Kim and J. Lee. *Antioxidants*, 2021;**10**:1-15.
- 22 I. Alam, S. Forid, M. Roney, F.F.M. Aluwi, M. Huq, and G. Zastrow. *Clinical Phytoscience*, 2020;**6**:35.
- 23 Y. Jang and E. Koh. *Food Science and Biotechnology*, 2019;**28**:337-345.
- 24 M.R. Khan, S.M. Hoque, KFB. Hossain, MAB. Siddique, MK. Uddin, and MM. Rahman. *Green Chemistry Letters and Reviews*, 2020;**13**:303-315.
- 25 R. Ravi and V. Krishnamurthy. *International Journal of Health Sciences & Research*, 2019;**9**:174-194.
- 26 C. Zhang, D. Liu, L. Wu, J. Zhang, X. Li, and W. Wu. *Foods*, 2020;**9**:1-14.
- 27 K. Roy, C. Sarkar and C. Ghosh. *Applied Nanoscience*, 2014;**5**:1-7.
- 28 J. Singh, T. Dutta, K-H. Kim, M. Rawat, P. Samddar and P. Kumar. *Journal of Nanobiotechnology*, 2018;**16**:84.
- 29 D. Mihaylova and A. Lante. *The Open Biotechnology Journal*, 2019;**13**:155-162.
- 30 S.U. Ganaie, T. Abbasi, J. Anuradha and S.A. Abbasi. *Journal of King Saud University-Science*, 2014;**26**:229-229.
- 31 S. Ahmed, M. Ahmad, B.L. Swami, and S. Ikram. *Journal of Advanced Research*, 2016;**7**:17-28.
- 32 M.B. Gawande, S.N. Shelke, R. Zboril and R.S. Varma. *Accounts of Chemical Research*, 2014;**47**:1338-1348.
- 33 V. Chikan and E.J. McLaurin. *Nanomaterials*, 2016;**6**:1-9.
- 34 M. Shkir, Z.R. Khan, M.S. Hamdy, H. Algarni, S. AlFaify and G. Zastrow. *S. Materials Research Express*, 2018;**5**:095032.
- 35 N. Dahal, S. García, J. Zhou, and S.M. Humphrey. *ACS Nano*. 2012;**6**:9433-9446.
- 36 S. Aryal, M.K. Baniya, K. Danekhu, P. Kunwar, R. Gurung, and N. Koirala. *Plants*. 2019;**8**:1-12.
- 37 Y. Sun, Z. Pan, C. Yang, Z. Jia, and X. Guo. *Molecules*. 2019;**24**:1775.
- 38 A. Ghasemzadeh, V. Omidvar, and H.Z. Jaafar. *Journal of Medicinal Plants Research*, 2012;**6**:2971-2976.
- 39 J. Musilová, J. Bystrická, J. Árvay, and L. Harangozo. *Potravinárstvo Slovak Journal of Food Sciences*, 2017;**11**:82-87.
- 40 M. Mavaei, A. Chahardoli, Y. Shokoohinia, A. Khoshroo and A. Fattahi. *Scientific Reports*, 2020;**10**:1762.